Major histocompatibility class I antigenic peptides derived from translation of pre-mRNAs generate immune tolerance

Ewa Maria Sroka, Mathilde Lavigne, Marika Pla, Chrysoula Daskalogianni, Maria Camila Tovar-Fernandez, Rodrigo Prado Martins, Bénédicte Manoury, Guillaume Darrasse-Jéze, Megane Nascimento, Sebastien Apcher, et al.

PNAS RESEARCH ARTICLE | CELL BIOLOGY

Major histocompatibility class I antigenic peptides derived from translation of pre-mRNAs generate immune tolerance

Ewa Maria Sroka[a,b], Mathilde Lavigne[b], Marika Pla[b], Chrysoula Daskalogianni[a,b], Maria Camila Tovar-Fernandez[a,b], Rodrigo Prado Martins[c], Bénédicte Manoury[d], Guillaume Darrasse-Jéze[e,f,g], Megane Nascimento[h], Sebastien Apcher[h,1], and Robin Fåhraeus[b,e,i,1,2]

Edited by Nahum Sonenberg, McGill University, Montreal, Canada; received May 19, 2022; accepted January 4, 2023

Antigenic peptides derived from introns are presented on major histocompatibility (MHC) class I molecules, but how these peptides are produced is poorly understood. Here, we show that an MHC class I epitope (SL8) sequence inserted in the second intron of the β-globin gene in a C57BL/6 mouse (HBB) generates immune tolerance. Introduction of SL8-specific CD8$^+$ T cells derived from OT-1 transgenic mice resulted in a threefold increase in OT-1 T cell proliferation in HBB animals, as compared to wild-type animals. The growth of MCA sarcoma cells expressing the intron-derived SL8 epitope was suppressed in wild-type animals compared to HBB mice. The β-globin pre-mRNA was detected in the light polysomal fraction, and introducing stop codons identified a non-AUG initiation site between +228 and +255 nts upstream of the SL8. Isolation of ribosome footprints confirmed translation initiation within this 27 nt sequence. Furthermore, treatment with splicing inhibitor shifts the translation of the pre-mRNA to monosomal fractions and results in an increase of intron-derived peptide substrate as shown by polysome profiling and cell imaging. These results show that non-AUG-initiated translation of pre-mRNAs generates peptides for MHC class I immune tolerance and helps explain why alternative tissue-specific splicing is tolerated by the immune system.

MHC class I antigen presentation | mRNA translation | immune tolerance

Significance

This work shows that non-AUG translation initiation of pre-mRNAs generates antigenic peptide substrates for MHC class I immune tolerance. The data show the origin of intron-derived peptides presented on MHC class I molecules and help to explain how the immune system tolerates alternative tissue-specific mRNA splicing. This work also offers a physiological explanation of previously reported global non-AUG-mediated translation initiation.

Peptides presented on major histocompatibility class I (MHC-I) molecules serve to distinguish between self and nonself and to allow the immune system to eliminate infected or transformed cells (1). CD8$^+$ T cells that react against self-peptides presented on medullar epithelial cells in the thymus are eliminated to allow tolerance against the host's own transcriptome (1, 2). There are approximately 20,000 protein-encoding genes with an estimated further 10-fold alternative splice variants of which many are expressed in a tissue-specific fashion (3). Still, it is not known how central immune tolerance against alternative splice variants is achieved, but the presence of intron-derived peptides on MHC-I molecules (4, 5) has opened the possibility that antigenic peptides are derived from pre-mRNAs. Furthermore, non-AUG-initiated translation products have been reported, but the physiological role of these is not known (6).

Canonical translation is initiated at an AUG codon as the ternary complex carries a methionine tRNA. However, previous studies have shown that the translation of a 3′ untranslated region (UTR) sequence initiated at a CUG generates antigenic peptide substrates, and global ribosome profiling reveals a vast number of non-AUG-initiated translation sites (6). The translation of MHC-I peptide substrates can be spatiotemporally distinguished from the synthesis of full-length proteins, suggesting that different translation events produce antigenic peptides and full-length proteins (7). There are different mechanisms of translation described that bypass cap-dependent initiation. The internal ribosome entry sites (IRES) and the repeat-associated non-AUG translation (RAN) both depend on RNA structures for ribosome entry. RAN translation of the C9orf72 is initiated from introns following GGGGCC repeat expansions and gives rise to peptides causing toxic aggregates, leading to amyotrophic lateral sclerosis (ALS) disease (8).

Exploiting the immune system for cancer treatments has emerged as a promising concept. Immune checkpoint inhibitors improve the host's own immune system to target tumor cells, and genetically modified CAR-T cells have successfully been used to treat different types of cancers such as leukemia and lymphoma. Recent successes using RNA vaccines against viral infections have boosted the hopes of also being able to generate cancer vaccines. These therapeutic approaches are dependent on the presentation of neoantigens on the MHC-I molecules. Understanding the origin of these peptide products not only offers new insights into some of the cell biological basics of how mammalians distinguish self from non-self but also open for new therapeutic intervention strategies based on controlling the production of neoantigens.

Author contributions: E.M.S., M.P., C.D., R.P.M., B.M., S.A., and R.F. designed research; E.M.S. and M.L. performed research; E.M.S., M.C.T.-F., and M.N. contributed new reagents/analytic tools; E.M.S., C.D., R.P.M., B.M., G.D.-J., S.A., and R.F. analyzed data; M.L. involved in all animal experiments and critical article's revision; M.P. concepted animal work and analysis, contributed to data and tools analysis and interpretation and critically revised the article; C.D. contributed to data analysis and interpretation as well as critical article's revision; M.C.T.-F. contributed to polysome profiling and microscopy analysis experiments and interpretation; R.P.M., B.M., and G.D.-J. contributed to the design of work and critical interpretation and article's revision; and E.M.S., S.A., and R.F. wrote the paper.

The authors declare no competing interest.

This article is a PNAS Direct Submission.

[1]S.A. and R.F. contributed equally to this work.

[2]To whom correspondence may be addressed. Email: robin.fahraeus@inserm.fr.

This article contains supporting information online at https://www.pnas.org/lookup/suppl/doi:10.1073/pnas.2208509120/-/DCSupplemental.

Published February 6, 2023.

In this study, we have addressed the origin of intron-derived antigens for the MHC-I pathway by introducing a $CD8^+$ T cell epitope in the intron of the murine β-globin gene. We show that non-AUG-initiated translation of pre-mRNAs generates peptides for the MHC-I molecules that give rise to immune tolerance.

Results

Intron-Derived MHC-I Antigenic Peptides Are Expressed and Presented In Vivo to Specific $CD8^+$ T Cells. The sequence encoding SIINFEKL (SL8) MHC-I epitope derived from ovalbumin antigen was inserted in the second intron of the β-globin gene in a CD45.1-positive C57BL/6 mouse expressing the Kb MHC-I molecule (HBB animals) (Fig. 1*A* and *SI Appendix*, Fig. S1). SL8 presented on Kb MHC-I is detected by $CD8^+$ T cells (OT-1) from transgenic animals expressing the corresponding CD45.2-positive SL8-specific T cell receptor (TCR) (2). Adoptive transfer of 2×10^6 OT-1 $CD8^+$ T cells labeled with CellTrace Violet to HBB animals followed by CD45.2 $CD8^+$ T cell isolation revealed an average of 2.5-fold increase in OT-1 cell proliferation, as compared to OT-1 cells injected in wild-type (WT) mice (Fig. 1 *B* and *C*). The β-globin forms part of hemoglobin, and RNA expression analysis confirmed pre-mRNAs carrying the SL8 sequence in several tissues with the highest levels in the bone marrow (BM), blood, and spleen. Low levels were observed in the lymph nodes and no detectable levels in the thymus or liver (Fig. 1*D*). Equal expression levels of full-length β-globin in murine splenic cells and BM were observed in HBB and WT animals (Fig. 1*E*). This confirms that SIINFEKL insertion in the intron did not affect the production of full-length β-globin protein in HBB mice.

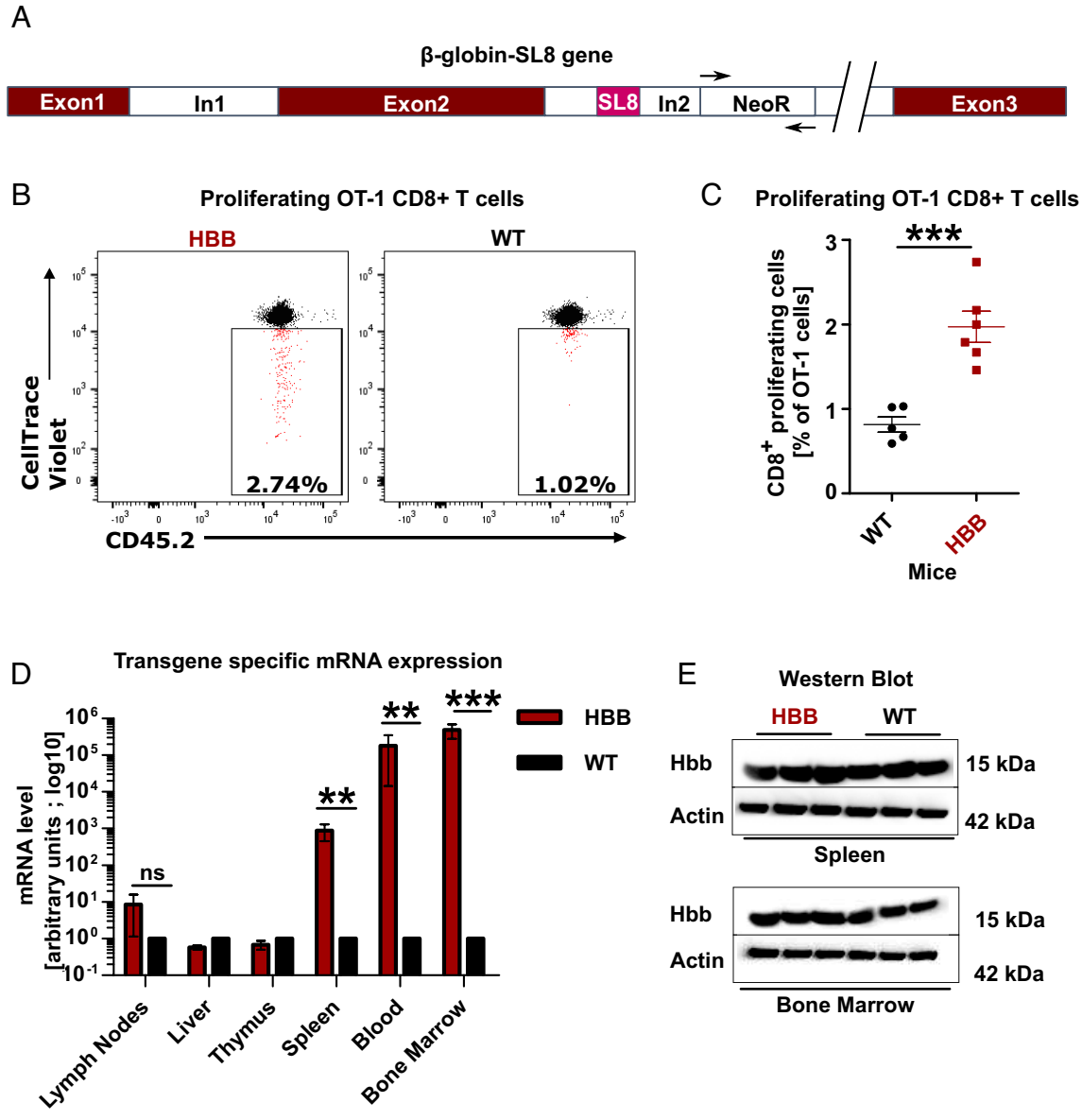

Fig. 1. The intron-derived MHC-I antigenic peptide (SL8) is expressed and recognized by specific $CD8^+$T cells in vivo. (*A*) A map of the HBB knock-in mice with the SIINFEKL encoding sequence (SL8) inserted in the second intron of the β-globin gene. The primers used for detection of the NeoR cassette are indicated. In 1: Intron 1; In 2: Intron 2. (*B*) FACS analysis of CellTrace violet-labeled CD45.2+ $CD8^+$ OT-1 T cells specific for the SL8-MHC I complex. When OT-1 cells detect the SL8 on Kb MHC-I molecules, they proliferate and gradually lose CellTrace violet label (9). Spleen cell analysis shows the percentage of CD45.2+ OT-1 T cells following injection in CD45.1+ HBB and CD45.1+ WT mice, 2.74% and 1.02% of total OT-1 T cells, respectively. (*C*) Graph shows data from 6 HBB and WT mice analyzed in five independent experiments (like in *B*) (***$P < 0.001$). (*D*) RT-qPCR confirms RNA expression of the HBB gene in indicated tissues with the highest levels in BM, blood, and spleen. The data were normalized against actin. (*E*) Western blot shows the expression of β-globin protein (Hbb) from splenic and BM cells from three HBB and WT animals.

HBB Mice Generate Reduced CD8$^+$ T Cell Response toward the SL8 Epitope. BM-derived dendritic cells (BMDCs) (1×10^6) were pulsed or not with SL8 peptide, treated with lipopolysaccharide (LPS), and injected intravenously to HBB and WT animals twice 7 d apart (Fig. 2*A*). This resulted in a significant decrease in the percentage of endogenous CD8$^+$ T cells expressing the SL8 peptide-specific TCR in peripheral blood lymphocytes (PBLs) after 10 d and the spleen after 12 d in HBB mice as compared to WT animals. No difference between HBB and WT mice was observed in BMDCs exposed to LPS alone (Fig. 2 *B*–*D*).

HBB Mice Are Tolerant to MCA205 Tumors Expressing SL8 from a Known Genomic Context. These data suggest that HBB mice are immune tolerant against the SL8 epitope. To test this further, we injected 5×10^4 MCA205 fibrosarcoma cells expressing the β-globin gene construct carrying the sequence encoding SL8 epitope in the second intron (β-globin-SL8) in WT or in HBB mice. Transduction efficiency was estimated to be over 95% (*SI Appendix*, Fig. S2*A*). Tumor growth from three independent experiments was evaluated 9, 16, and 21 d following subcutaneous (s.c.) injection. We observed a significant increase in tumor size in HBB animals after 21 d, as compared to WT (Fig. 2 *E* and *F*). There was no significant difference in the growth of MCA tumors expressing empty vector (MCA EV, *SI Appendix*, Fig. S2*B*). These data show that animals expressing the SL8 epitope from the second intron of the β-globin gene are immune tolerant toward this MHC class I-specific peptide.

Pre-mRNA Is Translated by Low-Molecular-Weight Polysomes. We next addressed the question of the RNA source from which the intron-derived SL8 peptide is translated. We carried out polysome

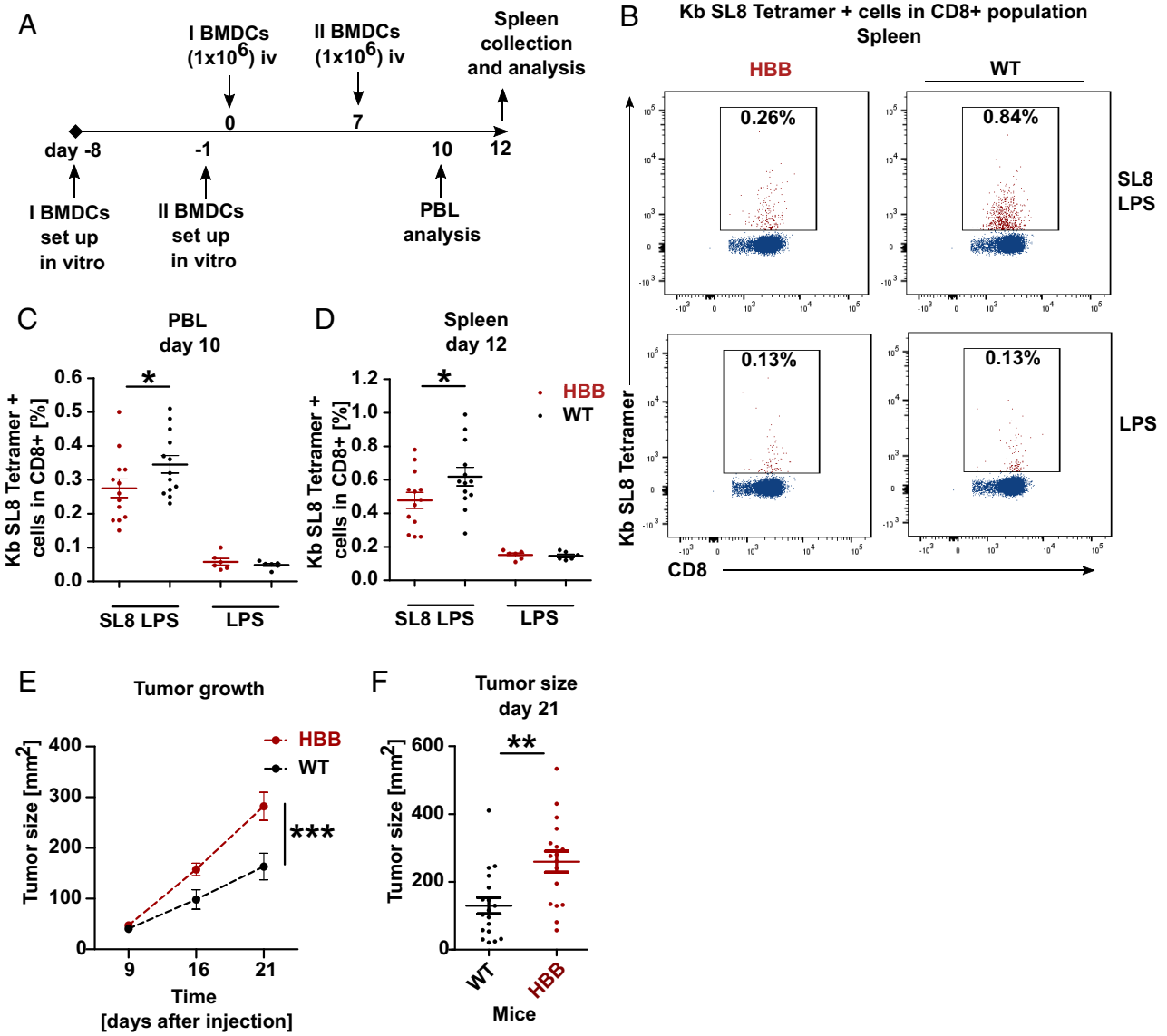

Fig. 2. HBB mice are immune tolerant against the intron-derived SL8 epitope. (*A*) 1×10^6 BMDCs pulsed with SL8 peptide, or not, and treated with LPS were injected intravenously (iv) in HBB and WT mice as indicated. (*B*) Following (*A*), FACS analysis shows percentage of CD8$^+$ Kb-SL8-positive tetramer cells specific for the Kb-SL8 epitope in splenic cells of HBB mice (0.26%) and WT mice (0.84%). (*C* and *D*) Percentage of Kb-SL8 tetramer+ cells in PBLs (*C*) or spleen (*D*) of HBB or WT animals at 10 or 12 d following injection, respectively (*$P < 0.05$). (*E*) 5×10^4 murine fibrosarcoma MCA205 cells stably expressing SIINFEKL in intron 2 of β-globin (β-globin-SL8) were injected subcutaneously (s.c.) in the flanks of HBB and WT mice and the tumor size was measured after 9, 16, and 21 d. Data represent tumor size (mm^2) following injection of MCA205 cells expressing the β-globin-SL8 (mean ± SEM) in HBB and WT mice over indicated time until the ethical end point is reached. (*F*) Postmortem measurements of MCA205 tumor size (like in *E*) at day 21. Graph represents individual data of three independent experiments with a total of 18 WT and 17 HBB animals (***$P < 0.0005$; **$P < 0.005$). Tumors expressing empty vector (MCA205 EV) grew similarly in both mice genotypes ($P > 0.05$) (see also *SI Appendix* Fig. S2).

fractionation on transiently transfected HEK293T cells (3) in order to identify the β-globin-SL8 mRNA distribution profile (Fig. 3*A*). Spliced and pre-mRNAs were detected using RT-qPCR with a combination of primer pairs corresponding to exons 1 and 2 as well as from sequences within intron 2 (SL8 and NeoR) (Figs. 3 *B* and *C* and *SI Appendix*, Fig. S3*A* and Table S1). Ribosome-associated pre-mRNAs were detected in the light polysomal fractions (fractions 3 and 4) (Fig. 3*D*), whereas spliced mRNAs were predominantly in the heavier fractions (fractions 7 and 8) (Fig. 3*E*). Treating cells with the splicing inhibitor isoginkgetin (ISO) resulted in an increase of nonspliced mRNAs in the lighter fractions and a subsequent decrease of spliced RNAs in the heavier fractions (Figs. 3*F* and *SI Appendix*, Fig. S3). ISO stimulates the synthesis of the SL8 antigenic peptide derived from minigenes but not from cDNAs, showing that ISO does not have off-target effects promoting antigenic peptide presentation (10).

Translation of the Intron-Derived SL8 Antigenic Peptide Substrate Starts from Non-AUG Codon. The SL8 epitope is encoded in the third frame of the β-globin-SL8 construct, and 276 nucleotides (nts) (+276) upstream of the SL8 sequence, there is an in-frame stop codon (Fig. 4*A*). Within this sequence, there are AUG codons in the same open reading frame (ORF), but their substitution by alanine had no, or minimal effect, on the synthesis of the SL8 peptide substrate (*SI Appendix*, Fig. S4*A*). Gradually introducing stop codons upstream of SL8 sequence prevented the synthesis of the SL8 epitope up to the position +228 (position no. 6). However, when a stop codon was introduced at position +255 (position no. 7) or +273 (position no. 8), SL8 expression was unaffected (Fig. 4 *A* and *B*). None of the mutations affected β-globin-SL8 pre-mRNA expression (*SI Appendix*, Fig. S4). This indicates that the synthesis of the SL8-carrying peptide substrates is initiated within these 27 nts between +228 and +255. To verify this, we carried out a modified ribosome profiling protocol in which HEK293T cells expressing the β-globin-SL8 construct were treated with harringtonin and cycloheximide (CHX) to maintain the ribosome in the position of initiation in order to generate ribosome-protected RNA fragments (ribosome footprint) (11). After RNAse treatment, the protected RNA fragments were isolated (Fig. 4*C*) and linked with stemloop primers (12) in the 3′ by reverse transcription, and qPCR confirmed the presence of the +255 to +228 sequence in the pool of ribosome footprints (Figs. 4*D* and *SI Appendix*, Fig. S4 and Tables S2 and S3). In this 27 nts sequence, there are two adjacent leucine (CUG) codons in frame with the SL8. CUG codons have been implicated in translation initiation of antigenic peptide substrates (7, 13), but introducing synonymous mutations in the third position in both codons (CUG > CUC) did not affect the expression of the SL8-carrying peptide substrate (*SI Appendix*, Fig. S4).

Inhibition of mRNA Splicing Increases Synthesis of Intron-Derived Peptides. To visualize the presence of intron-derived

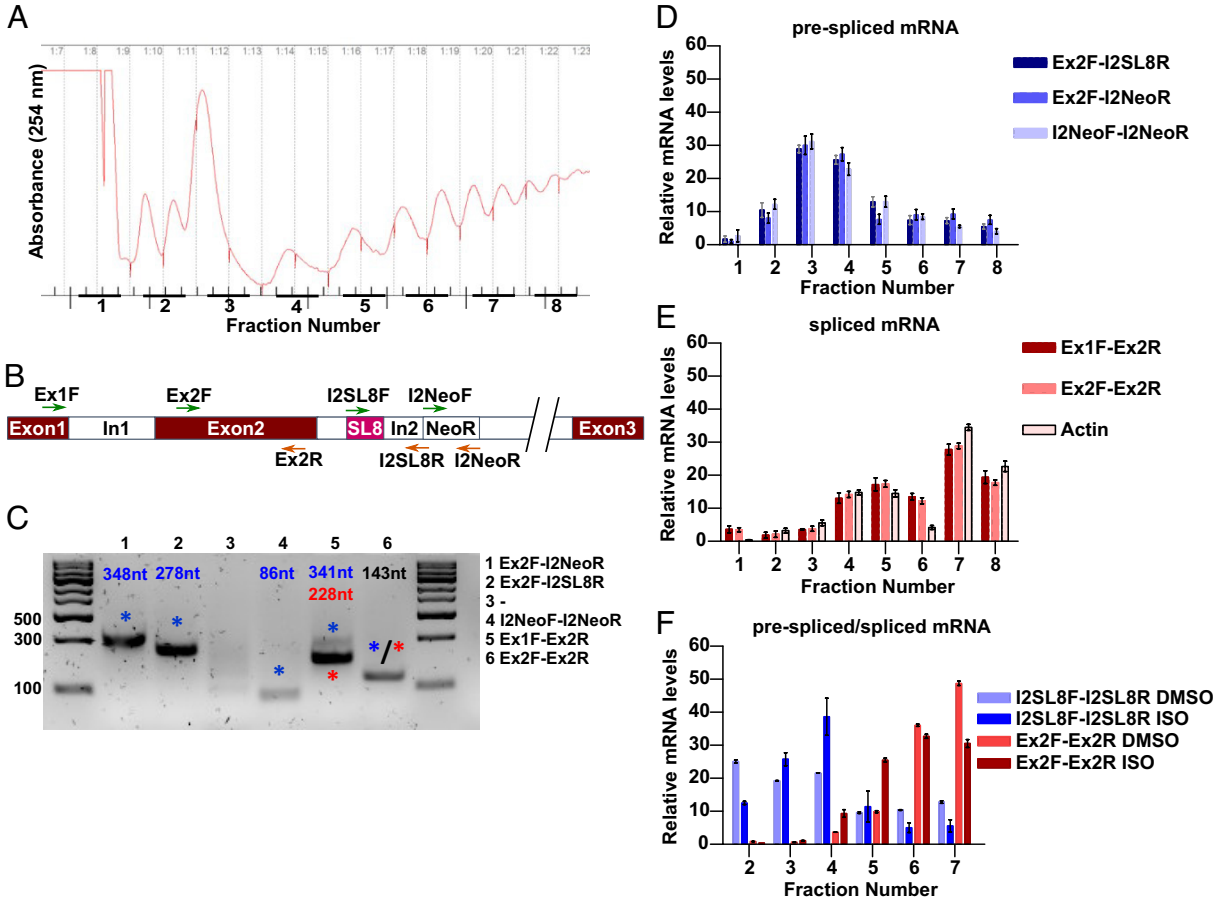

Fig. 3. Translation of the β-globin-SL8 pre-mRNA. (*A*) Graph shows the polysome profile from cells expressing the β-globin-SL8 construct. (*B*) Primers used for RT-qPCR are indicated. Forward primers are indicated by green and reverse primers by orange arrows. (*C*) Fractions three to eight were pooled, and RT-qPCR was performed using indicated primers and separation on agarose gel shows the estimated size of the PCR products. Blue and red asterisks indicate precursor and spliced products, respectively. Primers specific to exon 2 (Ex2F-Ex2R) do not distinguish spliced from pre-mRNA and, thus, the band is marked with blue and red. (*D* and *E*) The relative levels of precursor (*D*) or spliced (*E*) mRNAs using indicated primer pairs. (*F*) Treatment with splicing ISO shows decrease of spliced mRNAs in heavy polysome fractions and an increase of pre-mRNA in lighter fractions (*SI Appendix*, Fig. S3).

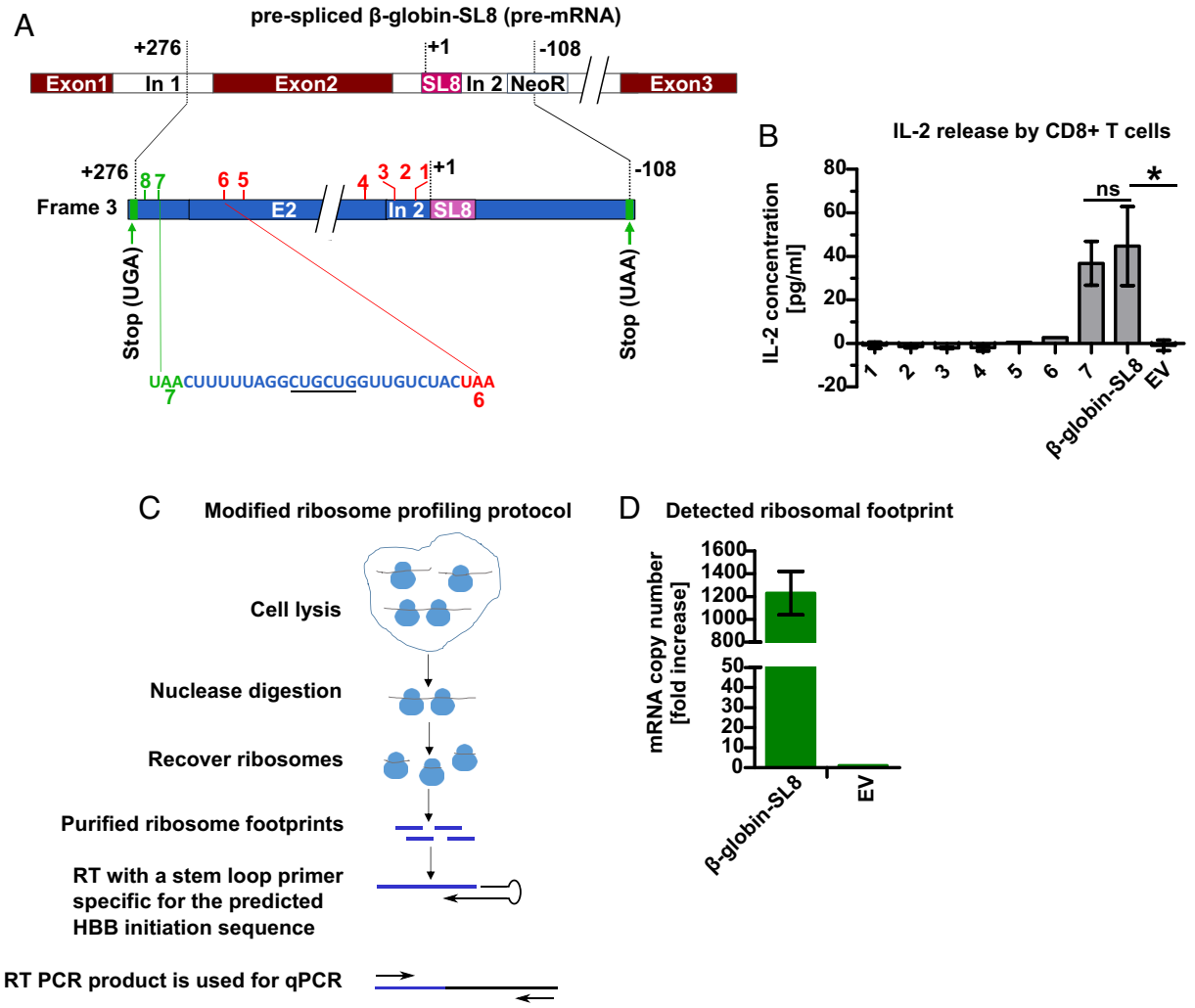

Fig. 4. Translation initiation of the SIINFEKL precursor peptide. (*A*) The sequence encoding SL8 epitope is in the third reading frame (blue), relative to the β-globin reading frame (red) and flanked by stop codons at nucleotide positions +276 and −108 relative to the SIINFEKL. (*B*) Stop codons (1 to 8) were introduced upstream of the sequence encoding SL8 epitope. OT-1 CD8$^+$ T cells were used to determine the synthesis of the SL8-carrying peptide substrate following expression of indicated β-globin-SL8 constructs in H1299 cells coexpressing the mouse Kb MHC-I molecule. The right graph shows the levels of IL-2 released by OT-1 CD8$^+$ T cells cocultured with transiently transfected cells expressing β-globin-SL8 constructs carrying indicated stop codons. Introducing stop codons at positions 1 to 6 (+228) prevented SL8 peptide synthesis (marked in red), but introducing a stop codon at +255 or +273 of SL8 (positions 7 and 8) (marked in green) had no significant effect on SL8 expression. This shows that initiation of translation takes place within the 27 nts sequence between stop codons 6 and 7 (+228 and +255, relative to SL8). Substituting the two adjacent CUG codons (underlined) within the 27 nt. sequence with CUC had no significant effect on SL8 production (*SI Appendix*, Fig. S4). (*C*) A modified ribosome profiling protocol was carried out to determine if the 27 nt. sequence harbors a ribosome initiation site. The cells were lysed under conditions that maintain the ribosome in the position of initiation using Harringtonin treatment followed by CHX (14). RNAse and DNAase were added to generate ribosome footprint, and ribosomes were isolated following ultracentrifugation for 22 h at 36,000 rpm. The ribosome-protected RNA fragments were isolated and stemloop primers were fused to the 3′ (Table S2). RT-qPCR was performed using primers corresponding to the 5′ of the predicted 27 nts initiation sequence and the stemloop (*SI Appendix*, Table S3). (*D*)The graph shows that the predicted 27 nt. sequence was included in the ribosome footprint of the pre (precursor) β-globin-SL8 RNA (EV: empty vector).

peptide products, we used the proximity ligation assay (PLA)(15) and a combination of affinity purified rabbit and goat sera raised against the N- or the C-terminal sequences of the SL8 peptide plus flanking intron sequences (Fig. 5*A* and *SI Appendix*, Fig. S5*A*). Treatment with 30 μM ISO for 20 h resulted in an increase in the amount of SL8-carrying peptide substrates, while at the same time immunohistochemistry showed less expression of the β-globin protein (Fig. 5*B* and *SI Appendix*, Fig. S5*B*). This shows that the synthesis of intron-derived SL8 peptide is more efficient from pre-mRNAs and, thus, is not derived from aberrant splicing products or a cryptic promoter. To test where translation of pre-mRNAs takes place, we carried out PLA using polyclonal goat antibodies against the C-terminal part of SL8 (FEKL) and rabbit polyclonal antibodies against ribosomal protein L5 (RPL5). Since intron-derived peptide substrates have a high turnover rate, cells were treated with (CHX) to freeze translation elongation and leave the nascent peptide attached to the ribosome. CHX treatment resulted in an increase in nuclear interactions between the nascent intron-derived peptide and RPL5 (Fig. 5*C*).

Discussion

The data presented show that pre-mRNAs are translated and that the peptide products are presented to the MHC-I pathway, offering an explanation to the origin of the vast amount of intron-derived peptides presented on MHC-I molecules. Since the number of spliced mRNAs is far greater than the number of genes, and since many splice variants are expressed in a tissue-dependent fashion, it has been an enigma why different peptide products generated by alternative splicing do not give rise to neoantigens and autoimmune reactions. Generating tolerance against peptides originating from the translation of pre-mRNAs can help explain

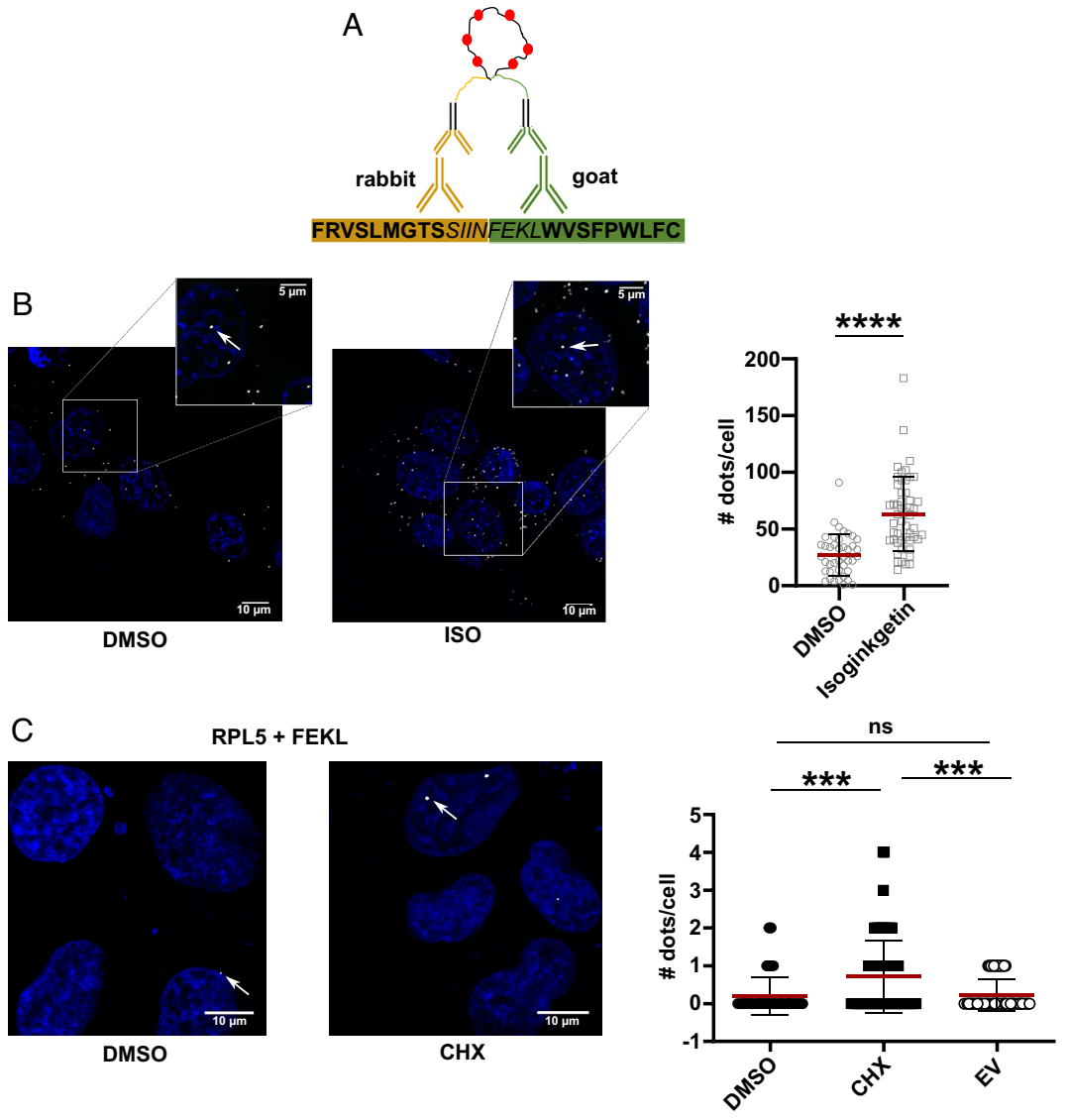

Fig. 5. Visualizing intron-derived MHC-I peptide substrates. (*A*) Rabbit and goat antibodies were generated using indicated peptides corresponding to the N-terminal half of SIINFEKL plus flanking intron sequence, or the C-terminal half plus flanking sequence, and (*B*) were used in PLA to visualize the expression of the intron-derived SL8 substrate in H1299 cells expressing the β-globin-SL8 construct (enlarged squares, white dots). Treatment with ISO increased the expression of intron-derived SL8-carrying peptides and reduced the amount of β-globin protein (*SI Appendix*, Fig. S5*B*), as compared to the DMSO control (*Left* images and *Right* graph). (*C*) Antibodies against RPL5 (rabbit) and FEKL (goat) were used in PLA to visualize the proximity of ribosomal protein and nascent peptide precursor in H1299 cells expressing β-globin-SL8 construct and treated with CHX or DMSO. The number of PLA dots was calculated using custom-made automated script in FIJI (****$P < 0.0001$ and ***$P < 0.001$).

how the immune system tolerates tissue-specific alternative splicing. The immune system has to use the same source of peptides for self-recognition in all tissues to minimize the risk of autoimmune reaction and, thus, the RNAs selected for encoding these peptide products need to have a common origin. This criterion is fulfilled by using pre-mRNAs. Moving an antigenic peptide sequence between introns and exons of a minigene, or introducing premature stop codons, has no significant effect on antigen peptide synthesis (16). Furthermore, the observation that splicing inhibitors stimulates the production of antigenic peptides derived from pre-mRNAs and not from ORFs encoded by cDNAs, further underlines that the origin of these products is from intact pre-mRNAs, and that cryptic RNA products are not the source (10).

The translation of introns from pre-mRNAs poses a problem from an mRNA translation point of view as there is no previous model to explain how this takes place. However, previous studies have shown that the synthesis of antigenic peptide substrates and full-length proteins is derived via spatiotemporally different translation events (7). For example, the transfection on an mRNA encoding an ORF harboring an antigenic peptide sequence resulted in the production of MHC-I peptides for up to 2 h following transfection, while the synthesis of the full-length protein continued for at least 8 h as long as the RNA was present (7). Furthermore, using the Rev-Rel system of HIV for RNA export, it was shown that forcing the export of an mRNA out of the nucleus increased the synthesis of the encoded full-length protein but reduced the production of antigenic peptide substrates (10). There are examples of alternative translation events and in the case of IRES, the preinitiation complex interacts directly with RNA structures and bypasses cap-dependent initiation. The non-AUG repeat (RAN) translation is another example in which RNA structures govern initiation and in the example of the C9orf72, the translation takes place on introns (8).

The antigenic peptide sequence (SL8) of the HBB mice is located in a different reading frame from the β-globin ORF, and gradually moving stop codons upstream of the SL8 prevented the

synthesis of SL8 peptide substrates until position +255 of the SL8 sequence at which it had no effect. A stop codon at +228 still prevented SL8 from being expressed, showing that translation of the SL8-encoding sequence starts within +228 to +255. The adapted RNA footprint shows that after treatment with harringtonine, that prevents translation elongation, there is a ribosome-protected RNA fragment corresponding to this sequence. There is no AUG within this sequence, and mutations of two adjacent CUG codons show that neither of these is being used for initiation, arguing that other non-AUG codons are used. Ribosome footprint has indeed shown that non-AUG initiation is common throughout the genome, and it is plausible that the physiological role of these initiations is the synthesis of MHC-I peptide substrates (6, 17). Indeed, translation initiation of antigenic peptide substrates from non-AUG codons has previously been shown using a CUG codon within a 3′ UTR (5, 13, 18). Furthermore, introducing synonymous mutations in leucine codons in two different mRNAs changed the expression of MHC-I peptide substrates, but not of the full-length protein (7). This shows that alternative translation initiation using AUG for full-length protein synthesis and non-AUG codons for generating antigenic peptide substrates can take place on the same ORF. Further analysis of the exact initiation site for the SL8 sequence within the β-globin gene will be difficult since it is likely that the translation initiation is guided by RNA structures and any mutation within this region might change this structure and thus, indirectly, affect initiation.

We used proximity ligation to show that the proximity of the nascent SL8 peptide and RPL5 is detected in the nucleus. Together with a previous study in which a nascent HA tag expressed from an intron was detected in the nucleus, these results are consistent with the notion that MHC-I peptides are synthesized during a pioneer round of translation (16). The RNA quality control of spliced mRNAs that precedes nonsense-mediated decay (NMD) is carried out by ribosomes, and it has been suggested that this can take place in the perinuclear space, but as pre-mRNAs are cotranscriptionally spliced, it is less likely that the synthesis of MHC class I peptides takes place in the perinuclear space (9, 14). This opens the possibility that there is a translation event taking place before NMD scanning and that it takes place in the nucleus. Nuclear translation remains controversial but has been suggested by different groups, and it is interesting to note that a cotranscription/translation event and nuclear peptide substrates with a high turnover rate in eukaryotic cells have been reported (16, 19–23). Ribosomal factors have also been detected at the site of nascent Pol II transcripts (24). One critical issue regarding nuclear translation has been the physiological role of the peptide product. The synthesis of antigenic peptide substrates might be one such physiological role that at the same time can also help explain the observations of global non-AUG-initiated translation (6). Some of the arguments against nuclear translation are based on the canonical translation producing full-length proteins, but in the case of intron-derived antigenic peptides, the mechanism of initiation is not canonical and, thus, the possibility that these are made in the nucleus has to be considered.

The observations that antigenic peptides are derived from noncanonical translation of pre-mRNAs will open for designing vectors that are optimized for producing antigenic peptide substrates for more efficient vaccines. It is also possible that knowing the origin of neoantigens can help predict the presentation of neoantigens in cells carrying somatic mutations and thereby help design CAR T cells. Another aspect is how the synthesis of MHC-I peptides is regulated. A recent report suggested that DNA damage induces the synthesis of MHC-I peptides from a pioneer round of translation (25). It is thus possible that the translation of pre-mRNAs is regulated, and it will be interesting to see if this is a target for tumor and viral immune evasion.

Materials and Methods

Mice. OT-1 $CD8^+$ T cells which expressed a TCR recognizing SIINFEKL-MHC(Kb) complexes from CD45.2 mice were used as donors of $CD8^+$ T cells in in vivo antigen presentation assays (2).

C57BL/6 HBB CD45.2 mice were generated in Ciphe's laboratories, Marseille, by introduction of SIINFEKL DNA sequence to intron 2 of β-globin gene in chromosome 7 via homologous recombination. Heterozygous ES cells were selected with neomycin and injected to blastocysts used in mice in vitro fertilization. Chimeric animals were bred into wt C57BL/6 CD45.2 and heterozygotes were backcrossed seven to nine times. The strain was later crossed with C57BL/6-Ly5.1 mice in order to obtain animals with CD45.1 alloantigen expressed on $CD8^+$ T cells.

All animal experiments were authorized and validated by the ethics committee Paris Nord/n°121 in compliance with the European directive and its transposition into French law (authorization APAFIS#19923 and APAFIS#32330).

Cell Culture and Transfection. H1299, MCA205, and HEK293T cell lines were cultured under standard conditions. Plasmid constructions, stable cell line generation, and quantitative RT-PCR (qRT-PCR) are described in *SI Appendix*.

RNA Analysis of Murine Organs.

Thymus, spleen, lymph nodes, liver. HBB and WT mice of 10 wk old were killed, and thymus, spleen, lymph nodes, and liver were collected, cut into two to three pieces, and snap frozen using liquid nitrogen. RNA extractions were performed according to the protocol provided by Qiagen RNeasy Mini Kit.

Blood and BM. Blood samples were collected from the submandibular vein of HBB and WT mice that were 6 mo old. After collection, the mice were killed by cervical dislocation and BM isolated from the femurs and tibias. RNA from blood and BM was isolated with Trizol LS and TRIZOL reagents according to the manufacturer's protocols.

In vivo antigen presentation. OT-1 CD45.2 mice were killed by cervical dislocation. Lymphoid organs were homogenized on a 70-μM cell strainer with PBS containing 5% FBS. $CD8^+$ T cells were purified with Mouse $CD8^+$ T cell Isolation Kit (MACS, Miltenyi Biotec) according to the manufacturer's instructions. $CD8^+$ T cells were labeled with cell-trace violet (CellTrace™ Cell Proliferation Kits, Invitrogen) according to the manufacturer's protocol and injected intravenously (i.v.) to C57BL/6-Ly5.1 HBB and WT mice (2×10^6 T cells/animal).

After 3 d, $CD8^+$ T cells were isolated from lymphatic organs as above (MACS, Miltenyi Biotec) and analyzed by flow cytometry on a CANTO II flow cytometer (BD Biosciences) using the following markers: CD45.2 (PE-Cy7, BD Pharmigen), Fixable Viability Dye eFluor 780 (Affymetrix eBioscience; APC-Cy7), and Cell Trace Violet (Life technologies, DAPI). Data were acquired using DIVA software and analyzed using FlowJo software version 8 (Tree Star). The percentage of proliferating T cells was considered for statistical analysis (26).

Tumor tolerance assay. WT or HBB mice were injected subcutaneously with 5×10^4 MCA205 mouse sarcoma cells stably expressing β-globin-SL8 or empty vector (EV). Tumor growth was measured over time at days 9, 17, and 21 or until an ethical point was reached. Tumors were extracted and measured postmortem.

BMDC generation and immunization assay. BMDCs from C57BL/6N WT were pulsed with SIINFEKL peptide (0.5 μg/10^6 cells/1 mL) together with LPS (1 μg/mL) for 2 h at 37 °C. Control cells were pulsed with LPS alone at the same concentration. The cells were resuspended in PBS prior i.v. injections to WT and HBB mice (1×10^6 cells/mice) on days 0 and 7. On day 10, blood samples (100 μL) were collected from the facial vein and PBL analyzed by FACS (*SI Appendix*). On day 12, all mice were killed by cervical dislocation and lymph nodes and spleens collected. Single-cell suspensions of 5×10^6 cells were prepared for FACS analysis (*SI Appendix*).

In vitro antigen presentation. Assay description is provided in *SI Appendix*.

Polysome profiling. Assay description is provided in *SI Appendix*.

Adapted ribosomal profile. Cells were lysed under conditions to maintain the ribosome in the position of initiation using Harringtonin treatment followed by CHX (11, 17). RNAse and DNAse were added to generate ribosome footprint, and the ribosomes were isolated following ultracf. at 36,000 rpm for 22 h. The ribosome-protected RNA fragments were isolated as described, and stem loop (SL) primers were fused to the 3′. SL primers were designed according to the

protocol (12). RT-qPCR was performed using primers corresponding to the 5′ of the predicted 27 nt. initiation sequence and the SL with the use of the thermocycler StepOne Real-Time PCR system (Applied Biosystems). The list of primers is described in *SI Appendix* Tables S2 and S3.

PLA. PLA has been described before (15). H1299 cells were grown on coverslips and transfected with indicated constructs for 24 h and treated with 30 μM isoginkgetin (Merck Millipore) for 22 h. The cells were fixed in 4% paraformaldehyde for 20 min before being permeabilized in PBS and 3% BSA containing 0.1% saponin. PLA was performed with the use of custom-made primary antibodies – rabbit anti-SIIN, goat anti-FEKL (Eurogentec), or rabbit polyclonal antibodies against ribosomal protein L5 (RPL5) were incubated in the same buffer overnight. After the cells were washed, PLA probes were added, followed by hybridization, ligation, and amplification according to the manufacturer's protocol (Duolink, Thermo Fisher). Then, immunofluorescence was performed using primary mouse anti-β-globin antibody and secondary anti-mouse Alexa488. The coverslips were mounted on slides using SlowFade diamond antifade mounting medium (Thermo Fisher) with Hoescht. PLA signal was analyzed by confocal microscopy followed by full-length β-globin detection by fluorescence microscopy. The number of PLA dots was quantified in H1299 cells with or without β-globin-SL8 immunofluorescence signal by a custom-made automated script in FIJI.

Splicing assay. Assay description is provided in *SI Appendix*.

Data, Materials, and Software Availability. All study data are included in the article and/or *SI Appendix*.

ACKNOWLEDGMENTS. This work was supported by INSERM, European Regional Development Fund (ENOCH, CZ.02.1.01/0.0/0.0/16_019/0000868), MH CZ – DRO (MMCI, 00209805), Cancerforskningsfonden Norr, Cancerfonden (160598), Vetenskapsradet and partially by the International Centre for Cancer Vaccine Science within the International Research Agendas program financed by the European Union under the European Regional Development Fund.

Author affiliations: [a]International Centre for Cancer Vaccine Science, University of Gdańsk 80-308, Gdańsk, Poland; [b]Institut National de la Santé et de la Recherche U1131, Institut de Génétique Moléculaire, Université Paris 7 75010, Paris, France; [c]Infectiologie, Santé Publique, Institut National de la Recherche Agronomique, Université de Tours, U1282, 37380 Nouzilly, France; [d]Institut Necker Enfants Malades, Institut National de la Santé et de la Recherche U1151-Centre National de la Recherche Scientifique U8253, Université Paris Cité, 75015 Paris, France; [e]Sorbonne Universite, Institut National de la Santé et de la Recherche, U959, Immunology-Immunopathology-Immunotherapy Laboratory F-75013, Paris, France; [f]Université de Paris, Faculté de Médecine Paris Descartes F-75006, Paris, France; [g]Sorbonne Universités Assistance Publique–Hôpitaux de Paris, Groupe Hospitalier Pitié-Salpêtrière, Département de Médecine Interne et Immunologie Clinique, Institut National de la Santé et de la Recherche 959 F-75013, Paris, France; [h]Institut Gustave Roussy, Université Paris Sud, U1015, 94800 Villejuif, France; and [i]Department of Medical Biosciences, Umeå University, Umeå 90185, Sweden

1. L. Klein, M. Hinterberger, G. Wirnsberger, B. Kyewski, Antigen presentation in the thymus for positive selection and central tolerance induction. *Nat. Rev. Immunol.* **9**, 833–844 (2009).
2. K. A. Hogquist *et al.*, T cell receptor antagonist peptides induce positive selection. *Cell* **76**, 17–27 (1994).
3. B. J. Blencowe, Alternative splicing: New insights from global analyses. *Cell* **126**, 37–47 (2006).
4. C. M. Laumont *et al.*, Global proteogenomic analysis of human MHC class I-associated peptides derived from non-canonical reading frames. *Nat. Commun.* **7**, 10238 (2016).
5. M. V. Ruiz Cuevas *et al.*, Most non-canonical proteins uniquely populate the proteome or immunopeptidome. *Cell Rep.* **34**, 108815 (2021).
6. N. T. Ingolia, L. F. Lareau, J. S. Weissman, Ribosome profiling of mouse embryonic stem cells reveals the complexity and dynamics of mammalian proteomes. *Cell* **147**, 789–802 (2011).
7. S. Apcher *et al.*, Major source of antigenic peptides for the MHC class I pathway is produced during the pioneer round of mRNA translation. *Proc. Natl. Acad. Sci. U.S.A.* **108**, 11572–11577 (2011).
8. K. M. Green *et al.*, RAN translation at C9orf72-associated repeat expansions is selectively enhanced by the integrated stress response. *Nat. Commun.* **8**, 2005 (2017).
9. F. Lejeune, Nonsense-mediated mRNA decay, a finely regulated mechanism. *Biomedicines* **10**, 141 (2022).
10. R. P. Martins *et al.*, Nuclear processing of nascent transcripts determines synthesis of full-length proteins and antigenic peptides. *Nucleic Acids Res.* **47**, 3086–3100 (2019).
11. N. T. Ingolia, G. A. Brar, S. Rouskin, A. M. McGeachy, J. S. Weissman, The ribosome profiling strategy for monitoring translation in vivo by deep sequencing of ribosome-protected mRNA fragments. *Nat. Protoc.* **7**, 1534–1550 (2012).
12. M. F. Kramer, Stem-loop RT-qPCR for miRNAs. *Curr. Protoc. Mol. Biol.* (2022), 10.1002/0471142727.mb1510s95.
13. S. R. Starck *et al.*, Leucine-tRNA initiates at CUG start codons for protein synthesis and presentation by MHC class I. *Science* **336**, 1719–1723 (2012).
14. J. E. Dahlberg, E. Lund, Does protein synthesis occur in the nucleus? *Curr. Opin. Cell Biol.* **16**, 335–338 (2004).
15. O. Söderberg *et al.*, Direct observation of individual endogenous protein complexes in situ by proximity ligation. *Nat. Methods* **3**, 995–1000 (2006).
16. S. Apcher *et al.*, Translation of pre-spliced RNAs in the nuclear compartment generates peptides for the MHC class i pathway. *Proc. Natl. Acad. Sci. U.S.A.* **110**, 17951–17956 (2013).
17. N. T. Ingolia, S. Ghaemmaghami, J. R. S. Newman, J. S. Weissman, Genome-wide analysis in vivo of translation with nucleotide resolution using ribosome profiling. *Science* **324**, 218–223 (2009).
18. C. M. Laumont *et al.*, Noncoding regions are the main source of targetable tumor-specific antigens. *Sci. Transl. Med.* **10**, eaau5516 (2018).
19. A. David *et al.*, Nuclear translation visualized by ribosome-bound nascent chain puromycylation. *J. Cell Biol.* **197**, 45–57 (2012).
20. F. J. Iborra, D. A. Jackson, P. R. Cook, Coupled transcription and translation within nuclei of mammalian cells. *Science* **293**, 1139–1142 (2001).
21. S. Baboo, P. R. Cook, "Dark matter" worlds of unstable RNA and protein. *Nucleus* **5**, 281–286 (2014).
22. P. R. Theodoridis *et al.*, Local translation in nuclear condensate amyloid bodies. *Proc. Natl. Acad. Sci. U.S.A.* **118**, e2014457118 (2021).
23. J. E. Dahlberg, E. Lund, E. B. Goodwin, Nuclear translation: What is the evidence? *RNA* **9**, 1–8 (2003).
24. S. Brogna, T. A. Sato, M. Rosbash, Ribosome components are associated with sites of transcription. *Mol. Cell* **10**, 93–104 (2002).
25. Y. Uchihara *et al.*, DNA damage promotes HLA class I presentation by stimulating a pioneer round of translation-associated antigen production. *Mol. Cell* **82**, 2557–2570.e7 (2022).
26. A. B. Lyons, S. J. Blake, K. v. Doherty, Flow cytometric analysis of cell division by dilution of CFSE and related dyes. *Curr. Protoc. Cytom.* **9** (2013), 10.1002/0471142956.cy0911s64.